

# Theoretical Predictions of $W\gamma$ and $Z\gamma$ Production in Run II

Doug Benjamin, Alfred Goshaw, Michael Kirby

*Duke University, Physics Department, Durham, North Carolina 27708*

Beate Heinemann, Helen Hayward

*University of Liverpool, Liverpool, UK L69 3BX*

Naho Tanimoto

*Okayama University, Okayama 700-8530, Japan*

## Abstract

A study of theoretical calculations of  $W\gamma$  and  $Z\gamma$  production from  $p\bar{p}$  collisions are presented. For  $W\gamma$  production, Standard Model predictions from four matrix element calculations: **WGAMMA**, **WGRAD**, **PYTHIA** and **COMPHEP**, are compared at the parton level. The full Monte Carlo event generation including initial state radiation and hadronization is simulated using the **WGAMMA** and **ZGAMMA** matrix element calculations followed by **PYTHIA** shower generation. These studies are used to determine the uncertainty in the Standard Model predictions for  $W\gamma$  and  $Z\gamma$  production including an estimate of higher order QCD corrections.

## 1 Introduction

The interest in  $W\gamma$  and  $Z\gamma$  production in  $p\bar{p}$  collisions arises from the sensitivity to the triple gauge-boson vertex. The value of this coupling is predicted from the electroweak  $SU(2)_L \times U(1)_Y$  symmetry and measurements provide fundamental tests of the non-Abelian nature of the Standard Model. Within the Standard model the photon couples at the  $WW\gamma$  vertex while the triple gauge-boson vertex for  $ZZ\gamma$  coupling is predicted to be zero. If the  $W$  and  $Z$  bosons were to have internal structure, deviations from these Standard Model predictions would be observed. Limits on any non Standard Model contributions to  $W\gamma$  and  $Z\gamma$  production are usually placed in terms of so-called anomalous couplings  $\Delta\kappa$  and  $\lambda$  which are zero in the Standard Model.

Both  $W$  and  $Z$  boson production can occur with direct photons from the bremsstrahlung of the initial state quarks and the boson's leptonic decay products. A full calculation of the  $p\bar{p}$  production of  $W$  and  $Z$  bosons with direct photons must include these radiated photons in addition to the those directly coupled to the  $W$  or  $Z$  boson vertex.

Measurements of the triple gauge-boson couplings have been made at LEP in  $e^+e^-$  collisions and at the Tevatron in Run I. We will extend these studies using the data from Run II. For these analyses, we need reliable Monte Carlo generators for the Standard Model predictions and the ability to introduce the effects of anomalous couplings. In this note we review recent matrix element calculations and evaluate their uncertainties. We investigate four matrix element Monte Carlo generators: **WGAMMA**, **WGRAD**, **PYTHIA** and **COMPHEP**. They are described in section 2. In section 3 we present a comparison of those programs at the parton level. We also establish the choice of electroweak parameters used to generate large parton level event samples.

For the generation of complete events, our choice of matrix element generator, **WGAMMA**, is coupled to **PYTHIA** for gluon radiation, hadronization and underlying event simulation. Finally

the events are passed through CDFSIM and processed through reconstruction version 4.9.1. Using these fully simulated events, a determination is made of the required parton-level generation cuts to guarantee full acceptance of the events used in our data analyses. This is discussed in section XXX.

In addition to the above leading-order matrix element predictions, we study NLO calculation to estimate the cross section k-factor and other changes in production dynamics. These studies are presented in Section 6. In Section 8, we summarize our recommendations for the generation of  $W\gamma + X$  and  $Z\gamma + X$  events from  $p\bar{p}$  collisions at a center of mass energy of 1.96 TeV.

## 2 Description of the programs

The electroweak tree-level Feynman diagrams for  $W\gamma$  production in  $p\bar{p}$  collisions are shown in Figure 1. The diagram in Figure 1 c) describes photon emision from the W boson triple gauge-boson coupling, while the other diagrams show photon radiation from quarks and leptons. In order to preserve gauge invariance, all four of the diagrams must be included in the production calculation. Figure 2 shows the corresponding tree-level diagrams for  $Z\gamma$  production.

We compare four Monte Carlo generators, **WGAMMA** (**ZGAMMA**), **WGRAD** (**ZGRAD**), **PYTHIA** and **COMPHEP**, which generate  $W\gamma$  ( $Z\gamma$ ) production including radiative W and Z boson final states. We first briefly review the technical implementations of these programs for the parton-level matrix element calculations. They treat the W and Z bosons with Breit-Wigner line shapes. The Z production includes the Drell-Yan continuum,  $Z/DY\gamma$ , which for brevity we refer to as  $Z\gamma$  in this note.

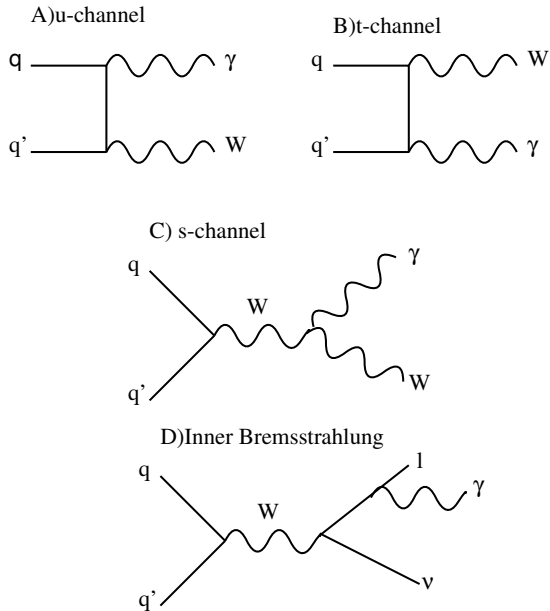


Figure 1: Tree level diagram for  $W\gamma$  production. Diagrams (A)-(B) represent initial-state radiation from the incoming quarks. Diagram (C) represents direct  $W + \gamma$  production and contains the vector boson self-interaction. Diagram (D) represents final state radiation or inner bremsstrahlung from the lepton and is known as radiative  $W$  decays.

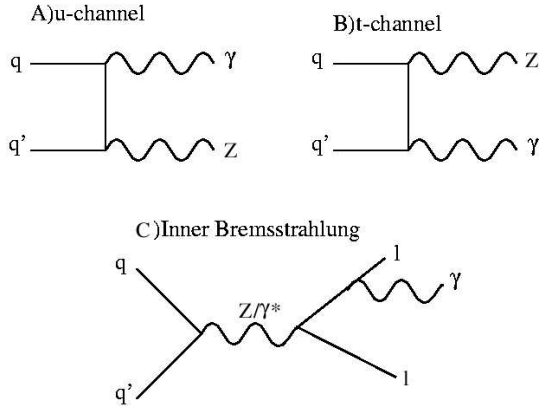


Figure 2: Tree level diagram for  $Z\gamma$  production. Diagrams (A)-(B) represent initial-state radiation from the incoming quarks. Diagram (C) represents final state radiation or inner bremsstrahlung from either final state lepton and is known as radiative  $Z$  decays.

## 2.1 WGAMMA

WGAMMA is a Monte Carlo matrix element generator provided by U. Baur and E.L. Berger [5]. The calculation is done at tree-level using electroweak helicity amplitudes for  $W\gamma$  production and radiative  $W$  boson decays, including all interference terms. An analogous program, ZGAMMA, is available for the generation of  $Z\gamma$  production with radiative  $Z$  boson decays. The event generation uses the Monte Carlo integration program VEGAS [6]. During 10 passes through the available phase space, the integration grid is allowed to map the peaks in the cross section. Areas with higher cross section are given a higher density of grid points. The grid is then frozen for additional passes, and during event generation further calls are made to the integration routine with the frozen grid. During the event generation, all events are recorded and the maximum weight for the sample of events is determined. Finally, a subset of events with unit weights are selected by comparing individual event weights to the maximum weight. An event is stored if its weight,  $w$ , satisfies :

$$w/w_{max} > \mathcal{R}[0;1] \quad (1)$$

where  $\mathcal{R}[0;1]$  donates a random number uniformly distributed between 0 and 1.

The WGAMMA and ZGAMMA calculations impose a minimum lepton-photon angular separation based upon the parameter,

$$\Delta R_{l\gamma} = [(\Delta\phi_{l\gamma})^2 + (\Delta\eta_{l\gamma})^2]^{1/2}$$

in order to suppress collinear photon emission. Infrared divergences are avoided by applying a minimum to the generated photon transverse momentum.

The WGAMMA and ZGAMMA event generation includes no QCD corrections to  $W$  and  $Z$  production. Therefore the matrix element generators have been interfaced to PYTHIA (version 6.203) to provide initial state gluon showers and hadronization, and a simulation of the underlying event. The WGAMMA (ZGAMMA) program includes mechanisms for introducing the anomalous coupling terms,  $\Delta\kappa_\gamma$  and  $\lambda_\gamma$  ( $h_{j0}^i, i=[\gamma, Z], j=[1..4]$ ).

## 2.2 WGRAD

The **WGRAD** program is a full NLO electroweak calculation of inclusive W boson production  $q\bar{q}' \rightarrow W^\pm \rightarrow l^\pm \nu$ , including the real photon contribution  $q\bar{q}' \rightarrow l^\pm \nu\gamma$  [7]. In the latter case, both initial state radiation (ISR) from the incoming quarks, final state radiation (FSR) from the charged lepton, and interference terms are included. **WGRAD** includes no QCD corrections to W production and decay. Also, anomalous coupling terms can not be introduced into the **WGRAD** calculation. This program was written by U. Baur. Details are discussed in [8]. **ZGRAD** is an analogous NLO electroweak program for inclusive Z boson production

The **WGRAD** calculation includes the real photon emision diagrams of **WGAMMA** , but is accurate down to low photon momenta. The program includes a photon collinearity cut, controlled by the parameter  $\delta_c$ , which is made on the angle between the charged fermion and the emitted photon in the parton-parton center of mass frame,

$$\cos \theta^* = 1 - \delta_c, \quad (2)$$

No additional cut on the separation ( $\Delta R_{l\gamma}$ ) is needed. A post production cut on the separation can be made, allowing comparisons in a limited region of phase space of the **WGRAD** and **WGAMMA** predictions. The **WGRAD** source code including the option of a **PYTHIA** interference, are currently reposed in the package **wgrad\_i**.

## 2.3 Pythia

The **PYTHIA** (`msub=20`) Monte Carlo generator program for  $W\gamma$  production includes matrix elements with the tree level u,t and s-channel diagrams and their inteference (Figure 1 A, B and C) , but does not properly include the inner bremsstrahlung diagram (Figure 1 D). Final state radiation off the W or Z boson decay particles can be introduced, but the correct interference terms are not included. **PYTHIA** does not have a provision for introducing anomalous W and Z boson coupling terms. The version **PYTHIA** 6.203 is currently part of the standard **cdfsoft2** package **generatorMods**.

## 2.4 COMPHEP

**COMPHEP** is a package for calculations of particle collision and decay in the lowest order of perturbation theory [4]. We use version 41.10 of the **COMPHEP** program. The package consists of two parts: symbolic and numerical. The symbolic part of **COMPHEP** calculates the squared matrix element terms from the Feynman diagrams input. The input diagrams are not limited to those in the Standard Model, but can include anomolous couplings. The C code produced from the symbolic calculation is then used in the numerical part to produce physical results. Once the symbolic results are interfaced into the numerical part, the matrix elements are convoluted with structure functions and beam spectra. Finally, the phase space integration is done using Vegas routines. **COMPHEP** then produces unweighted parton-level events that can be input into a shower Monte Carlo for complete event simulation.

Since **COMPHEP** starts its calculation with a symbolic step, the exact diagrams to be included in the calculation of  $W\gamma$  must be specified. So for the comparison between **COMPHEP** and **WGAMMA** , the exact same diagrams were used in both generators (see Figure 1). None of the higher order terms were input into the **COMPHEP** calculation, and there is no ISR or FSR gluon in the sample studied. **COMPHEP** does have the capability of varying the anomalous couplings. But the mechanism for including these additional terms requires the input of a new LaGrangian, and this option was not explored in these studies.

Some basic features of the four Monte Carlo programs are summarized in Table 1.

Table 1: Electroweak calculations of  $W\gamma$  production and the ability to change the anomalous couplings.

	Feynman Diagrams	anomalous coupling	EWK Order
WGAMMA	Fig. 1(A),(B),(C),(D)	yes	tree-level EWK $W\gamma$
WGRAD	Fig. 1(A),(B),(C),(D)	no	full NLO EWK $W$ inclusive
PYTHIA	Fig. 1(A),(B),(C)	no	partial tree-level EWK $W\gamma$
COMPHEP	Fig. 1(A),(B),(C),(D)	yes	tree-level EWK $W\gamma$

### 3 Comparisons at the parton level

In this section we present parton-level comparisons of the four Monte Carlo programs described in Section 2. We have tried to use exactly the same values for all the input parameters for these comparisons in order to check the consistency of the calculations.

The standard model parameters used for all these comparisons are given in Table 2. The parameter  $\sin^2 \theta_W$  is calculated from

$$\sin^2 \theta_W = 1 - \frac{M_W^2}{M_Z^2}. \quad (3)$$

We use CTEQ5L for the parton distribution functions with the factorization scale chosen to be the parton-parton center of mass energy. For WGAMMA and COMPHEP we set all anomalous couplings to their Standard Model value of zero.

Table 2: The standard model parameters used in the comparison of the Monte Carlo generators. For the electroweak parameters, inputs are shown in bold fonts, while the other EW parameters are derived.

Beam type	$p\bar{p}$
$\sqrt{s}$ [TeV]	1.96
PDF	CTEQ5L
$Q_f^2$	parton collision $\hat{s}$
$\alpha_s(M_Z)$	<b>0.127</b>
$M(W)$ [GeV]	<b>80.41</b>
$M(Z)$ [GeV]	<b>91.188</b>
$G_F$ [GeV $^{-2}$ ]	<b>1.6639</b> $\times 10^{-5}$
$\sin^2 \theta_W$	0.22242
$\alpha_{em}$	<b>1/132.43</b>
$\Gamma_W$ [GeV]	2.103
$\Gamma_Z$ [GeV]	2.514
$M(top)$ [GeV]	175

The generator level selection cuts applied to the event generation are summarised in Table 3. These cuts are looser than those used in the analysis of data (see CDF note 6366) so that all

relevant areas of phase space are explored when comparing different generators. The cuts on photon  $E_T$  and  $\Delta R_{l\gamma}$  are needed to avoid the divergence of the cross section due to the collinear and infrared singularities.

Table 3: Cuts for the generator level

	WGAMMA	WGRAD	PYTHIA	COMPHEP
Pseudorapidity cut for lepton $ \eta $	$< 10.$	$< 10.$	$< 10.$	$< 10.0$
Charged lepton $P_T$	no cut	no cut	no cut	1.0
neutrino $p_T$	no cut	no cut	no cut	no cut
$\gamma(E_T)$ [GeV]	$> 5.$	$> 5.$	$> 5.$	$> 5.$
Pseudorapidity cut for the photon $ \eta $	$< 10.$	$< 10.$	$< 10.$	$< 10.0$
$\Delta R(\text{lepton}, \gamma)$	$> 0.1$	*	$> 0.1$	$> 0.1$
Cluster transverse mass	no cut	no cut	no cut	no cut
Transverse mass( $l, \nu, \gamma$ )	no cut	no cut	no cut	no cut

### 3.1 PYTHIA versus WGAMMA

In order to compare PYTHIA and WGAMMA at the parton level, ISR and FSR gluon radiation are turned off in the PYTHIA generation. PYTHIA does not properly include the inner Bremsstrahlung of the W decay process as discussed in Section 2. So this was not included in the PYTHIA generation.

For this study, the  $\mu\nu$  decay of the W boson was generated. Figure 3 shows the 3-body invariant mass  $(\mu, \nu, \gamma)$  versus the 2-body invariant mass  $(\mu, \nu)$  for PYTHIA (left) and WGAMMA (right). In radiative W decays the  $\mu^\pm \nu$  pair and the photon form a system with invariant mass,  $M(\mu\nu\gamma)$ , close to  $M_W$ . For  $W\gamma$  production, on the other hand,  $M(\mu\nu\gamma)$  is always larger than  $M_W$  if finite-W-width effects are ignored. This difference suggests that  $\mu^\pm \gamma E_T$  events originating from radiative W decays can be separated by a  $M(\mu\nu\gamma)$  cut from  $W\gamma$  events which result in the same final state. Since the  $W\gamma$  process in PYTHIA does not include final state radiation, there is obviously no significant entries around 80 GeV/c<sup>2</sup> for 3-body invariant mass.

Since PYTHIA does not properly include W boson final state radiation, the predicted cross section and kinematic distributions will not be correct. Since we need a complete  $W\gamma$  generator, we will not use PYTHIA matrix elements for our predictions.

### 3.2 Comparison of WGRAD with WGAMMA

Since WGRAD is an inclusive W production generator, not every event contains a photon. In order to compare WGRAD and WGAMMA, we select events which have at least 3 particles in the final state: a lepton, a neutrino and a photon, for WGRAD Monte Carlo, i.e. at least one real photon emission is required. Since we are selecting events from the inclusive WGRAD sample, the distributions are normalized to the same area because an absolute normalization is impossible. This study will allow us to determine if the WGAMMA tree-level EWK calculation is sufficient for the photon  $E_T$  range above our experimental cut of 7 GeV.

Figure 4 shows the  $P_T$  spectra for the muon and the neutrino from the W decay. Figure 5 shows the  $\eta$  distributions for the lepton and the photon. Both the photon and the lepton are predominantly produced centrally but it is also seen that there is a significant portion for  $\eta_\gamma > 1$  such that it is important to include photons in the Plug calorimeter. Figure 6 shows the  $\Delta R$

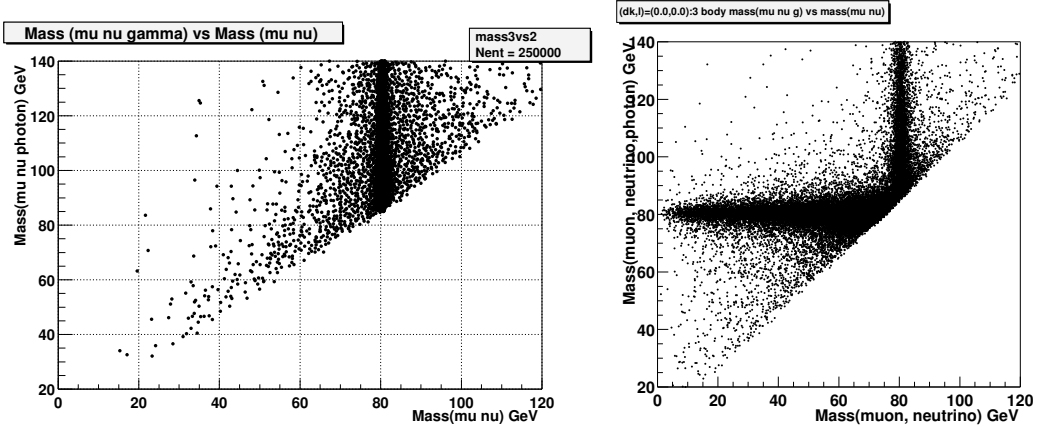


Figure 3: 3-body invariant mass  $(\mu, \nu, \gamma)$  v.s. 2-body invariant mass  $(\mu, \nu)$  plots for PYTHIA (left) and WGAMMA (right). As PYTHIA doesn't include final state radiation, there is no significant entries around  $80 \text{ GeV}/c^2$  for 3-body mass.

distribution and the invariant mass of the lepton and the neutrino. The  $\Delta R$  distribution is peaked at low values due to the dominance of the Bremsstrahlung diagram. This is also seen in the invariant mass distribution in which the tail below 80 GeV arises from the Bremsstrahlung diagram while the peak arises from the other three processes. We find good agreement for all these distributions between WGRAD and WGAMMA. In the histograms all plots have been normalised to equal area.

The matching distribution gives us confidence that the higher order electromagnetic corrections in WGRAD do not significantly change production in the regions of interest to our measurements, specifically low photon  $E_T$  and high  $\Delta R$ . Having verified that WGAMMA is accurate for our purposes, and since WGRAD does not include the option of introducing anomalous couplings, we choose WGAMMA as our default generator.

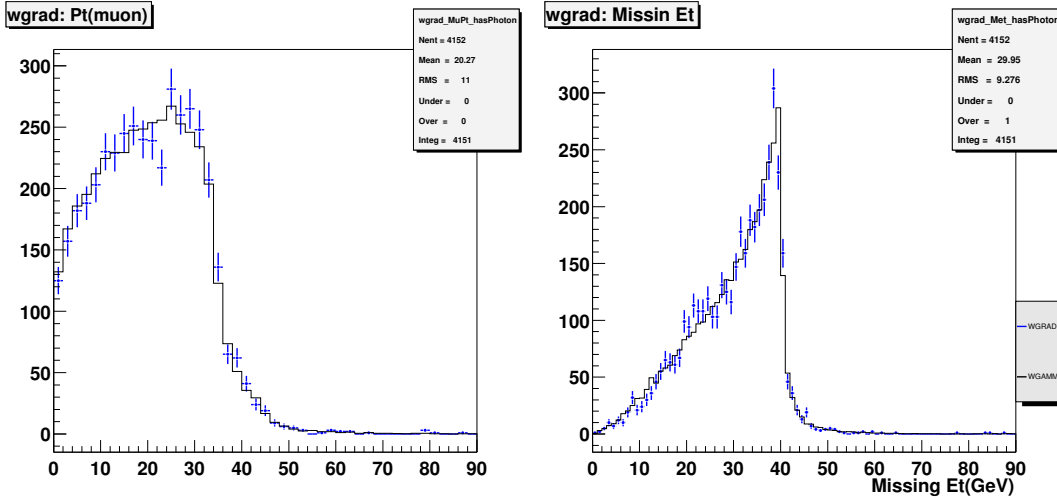


Figure 4:  $P_T$  spectrum of the muon (left) and neutrino (right) from WGRAD (crosses) and WGAMMA (histogram) Monte Carlo

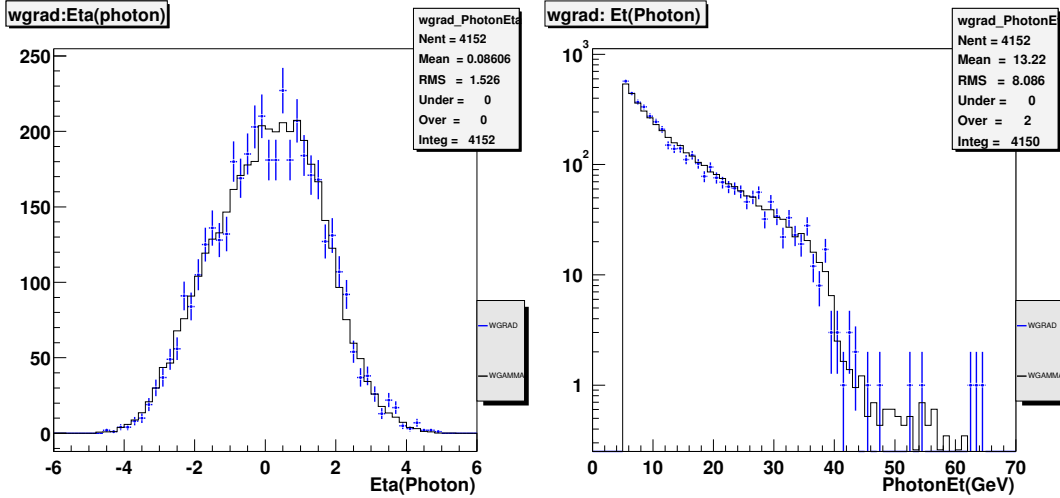


Figure 5:  $\eta$  of photon from WGRAD (dot) and WGAMMA (line) Monte Carlo.

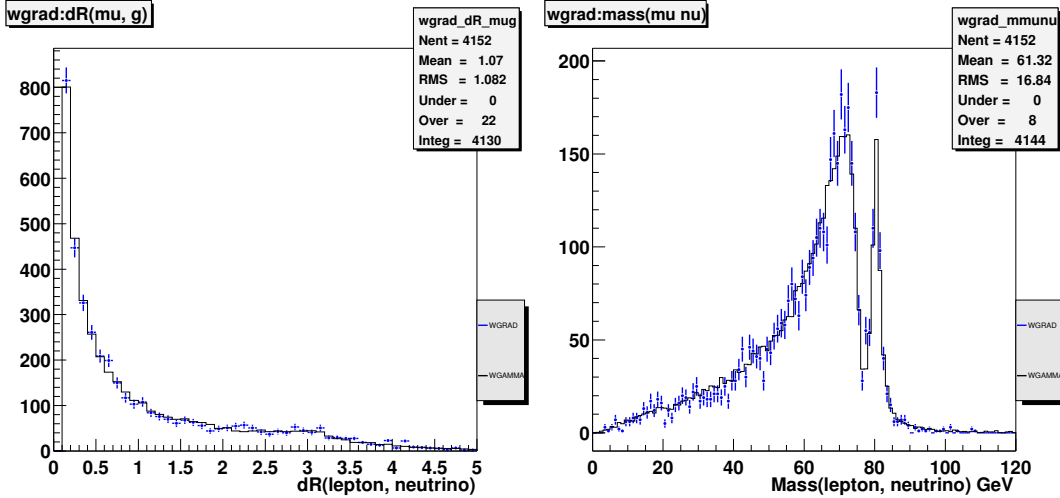


Figure 6:  $\Delta R(\text{lepton}, \gamma)$  from WGRAD (dot) and WGAMMA (line) Monte Carlo. Left is linear and right is log scale.

### 3.3 Comparison of COMPHEP and WGAMMA

As another check, we compare the predictions of the COMPHEP and WGAMMA event generators. COMPHEP contains all the terms for  $W\gamma$  production in the Standard Model, and so a direct comparison between COMPHEP and WGAMMA can be performed. The parameters in Table 2 were input into COMPHEP and 10000 unweighted events generated. These events were then analysed and compared with the events generated by WGAMMA. The plots in Figure 7-9 show the results of this comparison. There is generally good agreement between the WGAMMA and COMPHEP predictions. One problem we found with COMPHEP is that the version we used, generated events below the minimum photon  $E_T$  cut. This bug was reported to the COMPHEP authors, and has been fixed in future versions.

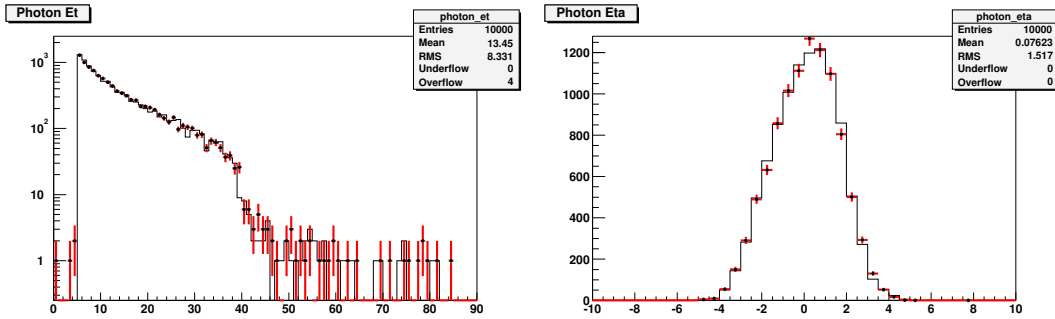


Figure 7: Photon  $E_T$  spectrum and  $\eta$  distribution from CompHEP and WGAMMA.

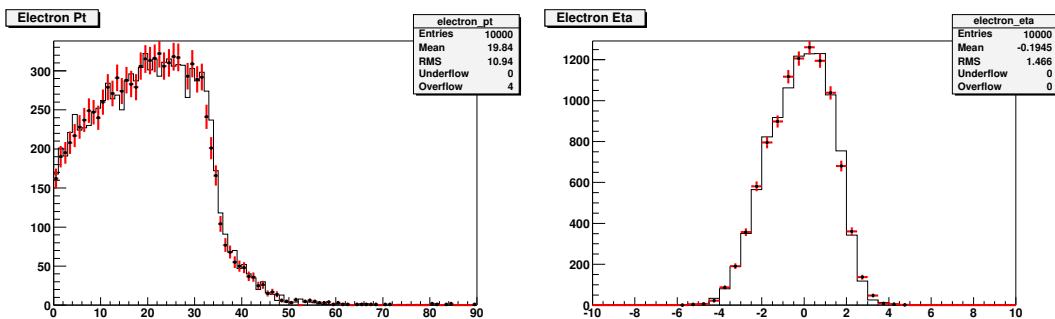


Figure 8: Electron  $P_T$  spectrum and  $\eta$  distribution from CompHEP and WGAMMA.

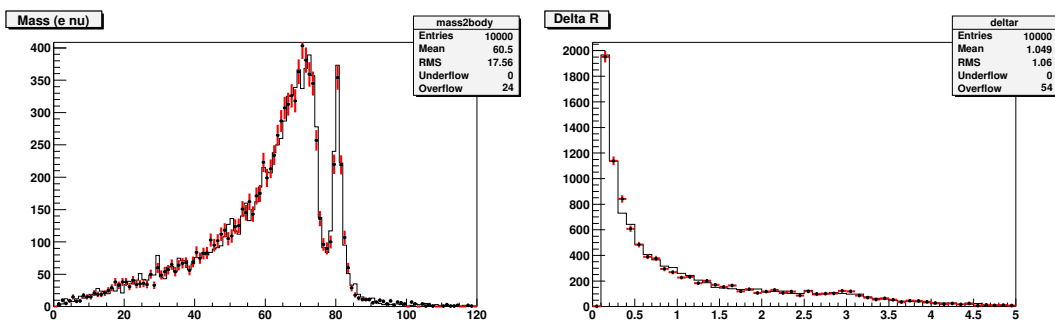


Figure 9: Invariant Mass of lepton and neutrino (left) and  $\Delta R(\text{lepton}, \gamma)$  distribution (right) from CompHEP and WGAMMA.

### 3.4 Additional Cross Section Comparisons

While the good agreement between normalized distributions is good, an additional check was done for the cross section calculation of each generator. For this comparison, an additional package `MCFM` was used even though no event distributions from `MCFM` were considered. The `MCFM` package of programs includes both LO (tree-level electroweak) and NLO (including first order  $\alpha_s$  corrections) for  $p\bar{p} \rightarrow W^+\gamma$  production. Considering only LO terms, the predictions should be the same as `WGAMMA`. Using the parameters in Table 2 and cuts in Table 3, the cross section predictions for  $W^+\gamma$  production are shown in Table 4. There is good agreement between the three generators, 2.6%. The small difference between `WGAMMA` and `MCFM` is attributed to a difference in input PDF (CTEQ5L vs CTEQ6M), while no source for the variation between `COMPHEP` and `WGAMMA` has been identified.

Table 4: Cross sections for  $p\bar{p} \rightarrow W^+\gamma \times \text{BR}(W^+ \rightarrow \mu^+\nu)$  from different generators. The generator level cuts are  $E_T^\gamma > 5 \text{ GeV}$  and  $\Delta R(\text{lepton}, \gamma) > 0.1$ .

generator	cross section [pb]
<code>WGAMMA</code>	19.2
<code>COMPHEP</code>	18.7
<code>MCFM</code>	19.0

### 3.5 Selection of Parton-Level Generator

We conclude that the `WGAMMA` and `ZGAMMA` event generators are the best options for Standard Model predictions of  $W\gamma$  and  $Z\gamma$  production. The parton level predictions for  $W\gamma$  production have been cross checked with `WGRAD` and `COMPHEP`. In addition, `WGAMMA` and `ZGAMMA` allow the introduction of the anomalous couplings of photons to the  $W$  and  $Z$  bosons. For complete event generation the parton level predictions are introduced into `PYTHIA 6.203` for gluon radiation, underlying event and hadronization.

While gathering information about these generators, we discussed the best choice of electroweak input parameters with U.Baur [11]. These are summarised in Table 5. These parameters have been used to generate large samples of  $W\gamma$  and  $Z\gamma$  events for the  $e$ ,  $\mu$ , and  $\tau$  decays of the  $W$  and  $Z$  bosons as described below. It should be noted that the value of  $\sin^2 \theta_W$  was fixed for both  $W\gamma$  and  $Z\gamma$  generation. While the mass of the  $W$  ( $Z$ ) was set to the PDG value for  $W\gamma$  ( $Z\gamma$ ) generation, and the mass of the  $Z$  ( $W$ ) calculated from  $\sin^2 \theta_W$ . This is why two values are listed for the mass of each vector boson.

## 4 Large Monte Carlo sample generation

Having chosen a generator to use, unweighted  $W + \gamma$  events were generated with `WGAMMA` using the set of cuts listed in Table 6. The cuts for the  $Z + \gamma$  events are listed in Table 7. These cuts were chosen to avoid the collinear divergences at low  $E_t^\gamma$  and low  $\Delta R$ . Concurrently, due to the large amount of CPU time necessary to simulate an event, the cuts must be far enough away from the analysis cuts to avoid efficiency turn ons and promotion from ISR. Since neither `WGAMMA` nor `ZGAMMA` contain any ISR in the calculation, a shower program must be used to simulate this effect. They were therefore interfaced with `Pythia 6.203`, and the Rick Field Tune

Table 5: The standard model parameters suggested by U. Baur and used for large scale **WGAMMA** and **ZGAMMA** MC production.

Beam type	$p\bar{p}$
$\sqrt{s}$ [TeV]	1.96
PDF	CTEQ5L
$Q_f^2$	parton collision $\hat{s}$
$\alpha_s(M_Z)$	<b>0.127</b>
$M(W)$ [GeV]	<b>80.41, 79.97</b>
$M(Z)$ [GeV]	<b>91.695, 91.1884</b>
$G_F$ [GeV $^{-2}$ ]	<b>1.6639 <math>\times 10^{-5}</math></b>
$\sin^2 \theta_W$	0.231
$\alpha_{em}$	<b>1/127.51</b>
$\Gamma_W$ [GeV]	2.103
$\Gamma_Z$ [GeV]	2.514
$M(\text{top})$ [GeV]	175

$A$  was applied. Also, since the decay of tau leptons is not done within **WGAMMA** , an interface to the cdfsoft2 package **TAUOLA** was written. The subsequent decay of the  $W\tau$  was done using this package. The  $\tau$  background is negligible for  $Z\gamma$  production. With these cuts and parameters, the large statistic samples listed in Table 8 were generated and run through detector simulation. For the purposes of determining the Standard Model prediction several cross sections must be calculated. These cross sections were measured using high statistics runs with **WGAMMA** and **ZGAMMA** . We show the cross section for the large MC samples generated, the kinematic region measured in the  $V + \gamma$  analysis, and for the cuts measured in the Run I exotics analysis. There are no cuts on  $\eta_\gamma$ ,  $\eta_{lep}$ , or  $P_t^{lep}$ . All cross sections reported are for both charges and include a  $k$ -factor of 1.34 as determined from Uli Baur's NLO **WGAMMA** program. The cross sections are listed in Table 9.

Table 6: Parton level cuts used for final  $W\gamma$  samples.

$ \eta_\gamma $	< 10.0
$ \eta_e $	< 10.0
$E_t^\gamma$	> 5.0GeV
$E_t^{lep}$	> 0.0GeV
$E_t^\nu$	> 0.0GeV
$\Delta R(\text{lep}, \gamma)$	> 0.2
min. mass gen.	> 1.0GeV/ $c^2$

## 5 Signatures for anomalous $WW\gamma$ couplings

The **WGAMMA** MC generator allows us to study the impact of non-zero values for  $\lambda$  and  $\Delta\kappa$  on individual distributions. The sensitivity is expected to be largest when the dominant Bremsstrahlung-diagram is suppressed. When this diagram is sufficiently suppressed, we get optimal sensitivity

Table 7: Parton level cuts used for final  $Z\gamma$  samples.

$ \eta_\gamma $	$< 10.0$
$ \eta_e $	$< 10.0$
$E_t^\gamma$	$> 5.0 GeV$
$E_t^l e p$	$> 0.0 GeV$
$\Delta R(l e p, \gamma)$	$> 0.2$
min. lep-lep mass	$> 20.0 GeV/c^2$
min. lep-lep-pho mass	$> 20.0 GeV/c^2$

Table 8: Large datasets generated with WGAMMA and submitted to tape.

Dataset	dataset_id	prod_id	Num Evts	Lum( $fb^{-1}$ )
$W^- \gamma \rightarrow e^- \nu \gamma$	ktop0e	ktop1e	106753	2.45
$W^+ \gamma \rightarrow e^+ \nu \gamma$	ktop0f	ktop1f	105619	2.43
$W^- \gamma \rightarrow \mu^- \nu \gamma$	ktop0m	ktop1m	105953	2.43
$W^+ \gamma \rightarrow \mu^+ \nu \gamma$	ktop0n	ktop1n	106846	2.45
$W^- \gamma \rightarrow \tau^- \nu \gamma$	ktop2t	ktop3t	100098	2.60
$W^+ \gamma \rightarrow \tau^+ \nu \gamma$	ktop2t	ktop3t	96558	2.57
$Z\gamma \rightarrow ee\gamma$	ktop2a	ktop4a	210208	17.8
$Z\gamma \rightarrow \mu\mu\gamma$	ktop2b	ktop4b	210208	17.8

 Table 9: Cross sections for final  $W\gamma$  and  $Z\gamma$  processes.

Process	$E_t^\gamma$	$\Delta R(l, \gamma)$	$\sigma(pb)$
$W\gamma \rightarrow e\nu\gamma$	5.0	0.2	43.4
$W\gamma \rightarrow e\nu\gamma$	7.0	0.7	18.7
$W\gamma \rightarrow e\nu\gamma$	25.0	0.7	3.0
$W\gamma \rightarrow \mu\nu\gamma$	5.0	0.2	43.1
$W\gamma \rightarrow \mu\nu\gamma$	7.0	0.7	18.6
$W\gamma \rightarrow \mu\nu\gamma$	25.0	0.7	3.0
$W\gamma \rightarrow \tau\nu\gamma$	5.0	0.2	37.9
$Z\gamma \rightarrow ee\gamma$	5.0	0.2	11.5
$Z\gamma \rightarrow ee\gamma$	7.0	0.7	5.3
$Z\gamma \rightarrow ee\gamma$	25.0	0.7	0.89
$Z\gamma \rightarrow \mu\mu\gamma$	5.0	0.2	11.5
$Z\gamma \rightarrow \mu\mu\gamma$	7.0	0.7	5.3
$Z\gamma \rightarrow \mu\mu\gamma$	25.0	0.7	0.89

to the triple gauge-boson diagram.

As we discussed in section 3.1, the three body invariant mass  $M(l\nu\gamma)$  cut is effective in distinguishing radiative W decays and initial state radiation from the more interesting  $W\gamma$  production. However, because of the invisibility of the neutrino,  $M(e\nu\gamma)$  can not be determined unambiguously and the minimum invariant mass or the cluster transverse mass [9]  $M_{CT}$  is more useful:

$$M_T^2(e\gamma; \not{E}_T) = [(M_{e\gamma}^2 + |\mathbf{p}_{T\gamma} + \mathbf{p}_{Te}|^2)^{1/2} + \not{E}_T]^2 - |\mathbf{p}_{T\gamma} + \mathbf{p}_{Te} + \not{E}_T|^2, \quad (4)$$

where  $M_{e\gamma}$  denotes the invariant mass of the  $e\gamma$  pair. The cluster transverse mass can be constructed for the  $W\gamma$  system by regarding  $P_z(\nu)$  as a free parameter and adjusting it to be minimal.

We compare the  $M_{CT}$  distribution for different choices of  $\lambda$  and  $\Delta\kappa$  and find that there is a detectable difference in the distribution. Additional sensitivity is seen in the  $\Delta R$  distribution at large  $\Delta R$  and the  $E_t^\gamma$  distribution at high  $E_t^\gamma$ . While the  $\Delta R$  and  $M_{CT}$  does have sensitivity, the greatest sensitivity comes from the  $E_t^\gamma$  distributions. Studies on the methodology and reach of anomalous limits are ongoing. This should be documented shortly in a note from Beate Heinemann and David Waters.

Using **WGAMMA** and **ZGAMMA**, samples with non-zero anomalous couplings were generated and processed through **CDFSIM** and **CDF** offline reconstruction version 4.9.1. This is the same prescription that was used for the SM sample previously discussed in Table 8. Slightly different generator level cuts were used since the phase space to be studied is well defined. The full list of parameters is listed in Table 10 and Table 11 with the changes listed in bold. The anomalous samples for **WGAMMA** were generated at 25 grid points with the values of  $\Delta\kappa$  and  $\lambda$  set to  $[-2, -1, 0, 1, 2]$ . The anomalous samples for **ZGAMMA** were generated at values of  $h_{30}^\gamma = [-8, -4, 0, 4, 8]$  and  $h_{40}^\gamma = [-1.0, -0.5, 0, 0.5, 1.0]$ .

Table 10: Parton level cuts used for **WGAMMA** samples with varied anomalous couplings.

$ \eta_\gamma $	$< 10.0$
$ \eta_e $	$< 10.0$
$E_t^\gamma$	$> 5.0 GeV$
$E_t^l ep$	$> \mathbf{15.0 GeV}$
$E_t^\nu$	$> \mathbf{15.0 GeV}$
$\Delta R(lep, \gamma)$	$> 0.4$
min. mass gen.	$> 1.0 GeV/c^2$

Table 11: Parton level cuts used for **ZGAMMA** samples with varied anomalous couplings.

$ \eta_\gamma $	$< 10.0$
$ \eta_e $	$< 10.0$
$E_t^\gamma$	$> 5.0 GeV$
$E_t^l ep$	$> \mathbf{15.0 GeV}$
$\Delta R(lep, \gamma)$	$> 0.4$
min. lep-lep mass	$> 20.0 GeV/c^2$
min. lep-lep-pho mass	$> 20.0 GeV/c^2$

## 6 Next to Leading Order Corrections

Since the **WGAMMA** event generator is a Leading Order (LO) program a Next to Leading Order (NLO) correction factor must be applied to the generated events. In order to determine a correction factor, we use Uli Baur's NLO program[16] to calculate a k-factor correction to  $W\gamma$  production at the Tevatron. To be exact, Baur's program is a Next to Leading Log (NLL) calculation taking into account only first order terms from QCD emission and not the second order electroweak terms. Since for large  $\Delta R$  the QCD correction dominates in proton anti-proton processes, this is the only correction that we apply to the LO program results. By taking the ratio of the NLL cross section to the LO cross section, a k-factor correction of 1.34 is measured. The k-factor was simplistically applied to the LO results by multiplying the LO cross section and using this corrected cross section to predict the SM signal. The k-factor was determined from the average of 10 large statistics runs. The maximal variation between the runs is quoted as the error,  $\pm 1\%$ . Additionally, similar QCD corrections are calculated for inclusive  $W \rightarrow l\nu$  production and the ratio of NNLO to NLO correction gives a correction of 3%. Since both final states ( $W\gamma$  and inclusive  $W$ ) are colorless, the QCD corrections should be comparable and so the NNLO correction is used as the error on the NLO k-factor. Combining the two errors, the total error on the k-factor is 3%.

Because the QCD correction involves the emission of an additional jet or gluon, the dynamics of the event are different in the NLO and LO calculations and the acceptance may vary. In order to study the effect, the acceptance for the analysis cuts at generator level was studied for the NLO and LO calculations. Since the NLO program cannot be unweighted using the traditional hit or miss method, the acceptance was measured as the ratio of the cross sections between the default cuts described in Table 6 and the central analysis cuts, for details see CDF Note 6601. The acceptance was then compared between the NLO and LO calculations. The acceptance for each was calculated using several runs with varying random seed, and then averaged together. The acceptance for the NLO program was 2.3% higher, and we then used this number as the error on the acceptance from the NLO correction. We chose to use this as the acceptance error instead of applying a correction because some ISR is applied during the Pythia fragmentation as discussed in Section 4.

## 7 LO Generator Systematics

The leading sources of systematic error in the event generation are PDF choice, online unweighting, factorization scale, k-factor and generation cut acceptance. The variations can appear as an error in the cross section or in the acceptance calculation. The systematics from the NLO k-factor were described in Section 6. Each of the other systematics were studied and the contribution of each is discussed below. The largest contribution comes from the choice of PDF and so it is discussed first.

The **WGAMMA** and **ZGAMMA** generators are LO and therefore we are limited to LO parton distribution functions (PDF). The possible PDF functions commonly used at CDF and considered here were MRST 72 – 76 and CTEQ5L. We choose the CTEQ5L PDF as the default at the recommendation of Uli Baur. In order to determine the systematic from this choice we calculated the LO cross section for the 5 MRST sets and the CTEQ5L. The MRST sets all returned a LO cross section clustered near 15.4  $pb$  for the cuts listed in Table 6. The CTEQ5L LO cross section was 16.2  $pb$ . The difference between the two was taken as the systematic error, 5%.

The factorization scale is the minimum  $q^2$  value calculated for photon emission with the **WGAMMA** and **ZGAMMA** programs. This setting is important as it also defines the maximum  $q^2$

value for the post-generation Pythia fragmentation. By default, the factorization scale is set to the collision  $\hat{s}$  and this value was used for large sample generation. The cross section was also calculated with four other values,  $2 \hat{s}$ ,  $1.5 \hat{s}$ ,  $2/3 \hat{s}$ , and  $1/2 \hat{s}$ . The variation in the five cross sections is taken as the systematic error from the factorization scale and is 2%. Additionally, the acceptance at generator level was measured for the different scales, but no variation was found. Therefore the systematic on the acceptance from the factorization scale is set to zero.

Finally, the effect of generation cuts on the acceptance was measured. In order to avoid the collinear and infrared divergences, a cut on  $\Delta R$  and the minimum photon  $E_T$  is applied during event generation. Since the Pythia factorization is applied after event generation and unweighting, some events generated below the analysis cuts can be promoted above minimum photon  $E_T$ . This effect was studied and is shown in Figure 7. The measured percentage of events promoted is less than 1%, and so the acceptance error from the generator cuts and unweighting is set to 1%.

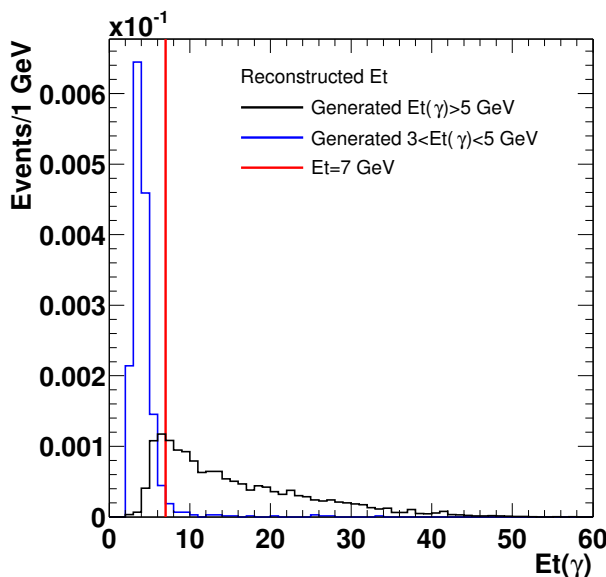


Figure 10: Reconstructed photon  $E_T$  for events generated at  $> 5 \text{ GeV}$  and between  $3 \text{ and } 5 \text{ GeV}$ . The number of events generated in the lower energy regime and promoted above the  $7 \text{ GeV}$  cut is less than 1% of the total number of events generated.

The total systematic error on the MC generation is shown in Table 12. The error on the cross section for  $W\gamma$  and  $Z\gamma$  is 7%. The error on the  $W\gamma$  and  $Z\gamma$  acceptance is 3%. These are the systematics used in the calculation of the cross section, and are not a comprehensive list of systematic errors for anomalous coupling limits or searches for gauge zeros. These systematic errors will be covered in subsequent notes discussing those analyses.

## 8 Conclusion

We have compared several different Monte Carlo generators for the  $lepton + \gamma + \nu$  final state. In order to study the properties of the  $WW\gamma$  and the  $ZZ\gamma$  vertex in the leptonic channel, it is necessary for the generator to have a fully gauge invariant calculation. In comparing the different generators, we found that for all generators containing the complete set of diagrams

Table 12: Systematic errors on the  $W\gamma$  and  $Z\gamma$  MC generation.

	$\delta\sigma$	$\delta A$
Factorization Scale	2%	0
Unweight	0	1%
PDF	5%	0
K-Factor	3%	2.3%
Total	7%	3%

similar results were produced. Since comparison between measured and predicted kinematic distributions will allow for a fit to anomalous couplings, variation of  $\Delta\kappa$ ,  $\Lambda$  and  $h_{j0}^\gamma$  was a necessity. While all of the programs considered produced results that were comparable, only the Baur **WGAMMA** and **ZGAMMA** programs had all of the capabilities along with a robustness due to their maturity. These generators were then used to generate samples that will serve as the standard Electroweak  $W\gamma$  and  $Z\gamma$  sample for Run 2a. Therefore we have chosen the **WGAMMA** and **ZGAMMA** programs for generation of our standard model electroweak predictions for  $W\gamma$  and  $Z\gamma$  production (see reference [15] for additional studies of the theoretical predictions). A k-factor of  $1.34 \pm 0.04$  is included for higher order QCD corrections. Comparisons of these predictions to data can be found in CDF note 6601.

## References

- [1] S. Jezequel, “Measurement of Charged Triple Gauge-Boson Couplings at LEP2”, Proceedings of ICHEP 2002, 525, 2002.
- [2] B. Abbott et al., “”, Phys. Rev. D 60, 072002 (1999).
- [3] D. Benjamin et al., “Event Selection in CDF Run I  $V + \gamma$  Analysis”, CDF note 5999
- [4] A.Pukhov, E.Boos, M.Dubinin, V.Edneral, V.Ilyin, D.Kovalenko, A.Kryukov, V.Savrin, S.Shchanin, A.Semenov, “CompHEP - a package for evaluation of Feynman diagrams and integration over multi-particle phase space.”, hep-ph/9908288
- [5] U. Baur and E.L. Berger, “Probing the  $WW\gamma$  vertex at the Fermilab Tevatron Collider”, Phys. Rev. D 41, 1476 (1990).
- [6] G.P. Lepage, Journ. Comp. Physics 27, 192 (1978).
- [7] U. Baur, S. Keller and D. Wackerlo, “Electroweak Radiative Corrections to  $W$  Boson Production in Hadronic Collisions”, Phys. Rev. D 59, 013002 (1999).
- [8] M. Lancaster and D. Waters, “A Monte Carlo Program for  $W$  Production with Electroweak Radiative Corrections”, CDF-Note 5240.
- [9] E.L. Berger, D. DiBitonto, M. Jacob and W.J. Stirling, “The minimum invariant mass - a technique for heavy quark searches at collider energy”, Phys. Lett. 140B, 259 (1984); V. Berger, A.D. Martin and R.J.N. Phillips, “Evidence for the t-quark in  $p\bar{p}$  collider data?” Phys. Lett. 125B, 339 (1983).

- [10] T. Sjöstrands, L. Lönnblad, S. Mrenna, P. Skands, “Pythia 6.2, Physics and Manual”, hep-ph/0108264, LU TP 01-21
- [11] Private communication with U. Baur
- [12] ETF and Muon group, “Baseline Analysis Cuts for High Pt Isolated Leptons”, [http://www-cdf.fnal.gov/internal/physics/ewk/hipt\\_lepton\\_baseline\\_cuts.html](http://www-cdf.fnal.gov/internal/physics/ewk/hipt_lepton_baseline_cuts.html)
- [13] A. Bhatti et al., “Generic Jet Energy Corrections for Run II data used for the Winter Conferences”. CDF note 6280
- [14] H. Hayward and B. Heinemann, “ Determination of the Probability of a Jet to fake an Isolated Photon”. CDF note 6363.
- [15] Henry Frisch and Chadd Smith, ”Predicted Cross Sections for W+Photon and Z+Photon Production”. CDF note 6057.
- [16] U. Baur, T. Han and J. Ohnemus, “QCD corrections to hadronic W gamma production with nonstandard W W gamma couplings,” Phys. Rev. D **48**, 5140 (1993) [arXiv:hep-ph/9305314].